Prediction of Tropospheric Wet-Component Range Error From Surface Measurements

P. S. Callahan
Tracking and Orbit Determination Section

A new formula relating the surface temperature and water vapor pressure to the wet-component range error is found based on an empirical exponential model of the vapor pressure as a function of height. It is pointed out that wet-component models based on the hydrostatic equation are probably invalid. The range error is proportional to the first power of the surface vapor pressure. The effective scale height varies with surface temperature and vapor pressure. Models are fit to 4 months of radiosonde measurements, and agreement to 1.4 cm (1 σ) is obtained. However, in 2 of the 4 months, the standard deviation of the daily values about the observed monthly average is only slightly greater than the rms difference between the model and the measurements.

I. Introduction

The wet component of the troposphere is a relatively small, but difficult to calibrate, error source. It is particularly troublesome at low elevation angles, where the zenith value ($\Delta R_W \sim$ 5–10 cm) is multiplied by a large factor. Many attempts have been made to determine the wet-component range error (see Ref. 1) from measurements made at the surface. Some progress has been made, but doppler residuals from Mariner 9 often show troposphere-like signatures (Ref. 2). Thus, it seemed useful to make another investigation of the problem.

The key element in any model of the troposphere is the distribution of water vapor with altitude. Berman (Ref. 3) assumed constant relative humidity to arrive at an expression relating the range error to the first power of the surface vapor pressure. Chao (Ref. 1) treated the water vapor as an adiabatic gas to derive $\Delta R_W \sim P_{0W}^{1.23}$. It will be shown in Section II that this derivation leads to inconsistencies. Here we follow Ref. 4 and assume that $P_W(z) = P_{0W} \exp(-az - bz^2)$, where z is distance above the ground. Using a linear temperature lapse rate, we integrate the refractivity to obtain the zenith range error.

In Section III, the new zenith range error expression is fitted to radiosonde measurements made during April, May, August, and September 1967 at Yucca Flats, Nevada. To fit the data, it is necessary to vary a and b in the above expression. The variations are correlated with temperature and surface vapor pressure: higher temperatures

result in smaller values for a and b. A linear fit for a and b is a good approximation to the data. The relationship between the parameters and the surface vapor pressure is less clear, but it appears that there is a limited range of pressures within which the exponential model applies.

In spite of the success of the model and the reasonable variation of its parameters with surface conditions, it must be noted that for April and August the rms deviation about the monthly average is only slightly greater than that about the model. Deviations of about 3 cm from both the average and the best model appear to occur at least once per month in the summer. This is consistent with the rms of 1.4 cm.

II. Refractivity Model Based on an Exponential Water Vapor Profile

The distribution of water vapor in the atmosphere is difficult to determine (Ref. 4). Theoretically, it obeys a turbulent diffusion equation with complicated boundary conditions, depending on the local surface conditions. The turbulent diffusion coefficient depends on wind velocity and other factors. Despairing of computing the water distribution from first principles, Ref. 4 states that the water vapor pressure distribution in western Europe has been found empirically to obey

$$P_W(z) = P_{0W} \exp(-az - bz^2) \tag{1}$$

where z is height above the ground, P_{0W} is the surface vapor pressure, and $a = 0.288$, $b = 0.0480$. Below, we will speak of the parameters a and b in terms of scale heights—their inverses. The effective scale height ($P \propto \exp(-z/d)$) corresponding to the above a and b is $d \sim 3.7$ km.

In view of the supposed difficulty in calculating the water vapor distribution, a comment on the work of Chao (Ref. 1) is needed. Chao used the hydrostatic equation

$$\frac{dP_W}{dz} = -\rho_W g \tag{2}$$

where g is the gravitational acceleration and ρ_W is the density of water vapor; a linear temperature lapse rate α, so that

$$T(z) = T_0(1 - \alpha z) \tag{3}$$

and the adiabatic law

$$P_W = D\rho_W^{\gamma} \tag{4}$$

where γ is the ratio of specific heats, to derive a relation between ΔR_W and P_{0W}. He used the measured value of the lapse rate α ($\alpha = 6$–8 K/km) with the measured value of γ for water ($\gamma = 1.3$), and D as an empirical parameter to fit data.

However, it is possible to derive γ and D in terms of α, so the above procedure is not internally consistent. A simple calculation for dry air using the adiabatic law and the measured γ for air (1.4) leads to a computed lapse rate of about 10 K/km, much higher than observed. Thus, the atmosphere does not behave in an adiabatic way. If one uses Eqs. (2) and (3), and the ideal gas law, a relation of the form of Eq. (4) can be obtained, with an effective γ expressed in terms of α. First, one derives (Ref. 3)

$$P(z) = P_0[T(z)]^{g/\alpha R} \tag{5}$$

where R is the universal gas constant divided by the molecular weight of the gas. Then the ideal gas law is used again to eliminate T from Eq. (6) and give

$$P = \left(\frac{P_0}{R^{g/\alpha R}}\right)^{1/(1-g/\alpha R)} \rho^{1/(\alpha R/g-1)} \tag{6}$$

Now D is a derived quantity and cannot be adjusted to fit data. The effective γ is 1.4–1.6 for water, much in excess of the true adiabatic index 1.3.

The real culprit in the above derivations is probably Eq. (2). While the dry part of the atmosphere ($\sim 99\%$) is in hydrostatic equilibrium, the partial pressure of water vapor is controlled by the local number density of water molecules. This quantity is determined by convection (wind) and need not be in hydrostatic equilibrium. Thus, Eq. (2) does not give the correct vapor pressure as a function of height, and derivations based upon it should be viewed with suspicion.

The pressure model of Eq. (1) is empirical, and the parameters given are for Europe, but it was thought useful to use it to compute the wet-component range error and test whether the form is valid. Comparison with data from various places and times could then be used to obtain the appropriate values of a and b for DSN stations.

The range error due to water vapor is given by (Ref. 1):

$$\Delta R_W = A\int_0^H \frac{P_W(z)}{T^2(z)}\,dz \tag{7}$$

where $P_W(z)$ is the partial pressure of the water vapor and $A = 0.373 \times 10^{-2}$ if ΔR_W is in centimeters and P_W in New-

tons per square meter; H is the height at which the water vapor vanishes. Empirically, H is in the range 7–10 km, but the exact value used makes no difference to the result. A linear temperature lapse rate is a good approximation to the observed temperature profile up to 7–10 km. Thus, the range error is given by

$$\Delta R_W = A\int_0^H \frac{P_{0W}\exp(-az-bz^2)}{T_0^2[1-(\alpha z/T_0)]^2}\,dz \tag{8}$$

Since $\alpha z/T_0 \lesssim 0.2$ up to 10 km, the denominator may be expanded. The resulting expression can be integrated easily to give the relation between P_{0W}, T_0, and ΔR_W, viz.,

$$\begin{aligned}\Delta R_W = {} & \frac{AP_{0W}\exp(a^2/4b)}{T_0^2\sqrt{b}} \\ & \times\left\{\left(1+\frac{\alpha a}{2T_0 b}\right)\frac{\sqrt{\pi}}{2}\left[\operatorname{erf}\left(\sqrt{b}\,H+\frac{a}{2\sqrt{b}}\right)\right.\right. \\ & \left.-\operatorname{erf}\left(\frac{a}{2\sqrt{b}}\right)\right]+\frac{\alpha}{T_0\sqrt{b}}\left[\exp\left(-\frac{a^2}{4b}\right)\right. \\ & \left.\left.-\exp-\left(\sqrt{b}\,H+\frac{a}{2\sqrt{b}}\right)^2\right]\right\}\end{aligned} \tag{9}$$

where erf is the error function

$$\operatorname{erf}(x) = \frac{2}{\sqrt{\pi}}\int_0^x \exp(-y^2)\,dy$$

which may be looked up in mathematical tables.

The sensitivity of Eq. (9) to a and b cannot be computed analytically because of the error functions. However, computer runs show that it is not overly sensitive and that $d\Delta R_W/\Delta R_W \cong 1/2\,(da/a)$ or $\cong 1/2\,(db/b)$, i.e., percentage changes map less than 1 to 1. Equation (9) allows a, b, and H to be functions of P_0 and T_0. Analytical fits are, of course, impossible, but comparisons of many different evaluations of Eq. (9) to observations allow the trends to be established.

For the nominal values of a (0.248 km^{-1}), b (0.048 km^{-2}), α (7 K/km), H (10 km), and T_0 (300 K), Eq. (9) reduces to

$$\Delta R_W = \frac{1.15\times 10^{-2}\,P_{0W}\,(\mathrm{N/m^2})}{(T_0/300\,\mathrm{K})^2}\ \mathrm{cm} \tag{10}$$

Typical water vapor pressures are in the range 4–15 $\times 10^2$ N/m^2, and temperatures range from 290–310 K. Zenith wet-component range errors are typically 4–15 cm, in agreement with Eq. (10).

III. Comparison of Model to Radiosonde Observations

Radiosonde measurements of the troposphere were obtained twice daily, at 0000 and 1200 UT, during most of 1967 at Yucca Flats, Nevada. Instruments carried aloft by a balloon measured the temperature and relative humidity as a function of height (pressure). The data were numerically integrated using Eq. (7) to find the wet-component range error.

Chao (Ref. 1) found that data obtained at 1200 UT (0400 local) do not give good results when used for surface predictions of ΔR_W. He points out that a temperature inversion invalidates the linear temperature lapse in Eq. (3). Thus, only data at 0000 UT (1600 local) were used. Two 7-week segments were found for comparison purposes. The first segment extends from April 10 to May 29; data for April 19 and May 4 and 21 are missing. The second segment, shown in Fig. 1, extends from August 6 to September 23; data for August 9 and 18 are missing. The figure contains the wet-component range error (ΔR_W, cm), the ground-level water vapor pressure (P_{0W}, N/m^2), the ground-level temperature (T_0, °C), the relative humidity (RH, %), and the height at which the contributions to ΔR_W cease ($H_{\max}$, km) plotted against date.

Table 1 lists the runs used to compare to the data and the temperature and pressure ranges in which they were found to apply. Two models are plotted with the data in Fig. 1—the best run for each month individually and the overall combination model given by the temperature and pressure ranges in Table 1.

The temperature and pressure ranges were found by a trial and error fit of a number of runs with different values for the parameters a and b to the 4 months of data described above. Recall that Run I was suggested to fit data in Western Europe; note that the temperature range in which it applies is probably typical of summer in Europe. The temperatures given in Table 1 are accurate to only about ±2°C. However, except for the special cases involving very high and low vapor pressures (Runs VIII and XII), the parameters $1/a$ and $1/b$ are well represented by linear functions of temperature. These functions are

$$\begin{aligned}\frac{1}{a} &= 1.4 + 0.078T\,(^\circ\mathrm{C}) \\ \frac{1}{b} &= 8.7 + 0.43T\,(^\circ\mathrm{C})\end{aligned} \tag{11}$$

Equation (9) and Eqs. (11), with the two exceptions noted above, form a simple and accurate model of the wet-component zenith range error.

The accuracy of the tropospheric model is summarized in Table 2. Each month's data are given individually along with statistics of the run which best fits that month and the combination model given by all of Table 1. Table 2 shows that the combination model is superior to any single run. Note that in April and August the monthly average is a better fit than a single run, and the combination model is barely better than the average in April. The work of Thuleen and Ondrasik (Ref. 5) shows that the monthly average should provide as good calibrations as the model for the months of December through April at the Goldstone stations. Models are the most useful in the spring and fall, when tropospheric conditions fluctuate a good deal. If the April data are ignored, the combination model has an rms deviation from the data of 1.52 cm.

The variation of the model parameters with temperature and pressure is interesting. As the temperature increases, so does the effective scale height, from about 2.6 km at 10°C to about 4.2 km at 35°C. Such a variation is expected for a gas in thermal equilibrium under the influence of gravity. However, the measured values of H_{max} (the height at which the contributions to ΔR_W cease) show only a rough winter–summer correlation with temperature. Furthermore, the special Model XII needed for low surface vapor pressures has by far the highest scale height, but the data of Fig. 1 show lower values of H_{max} at the times when this model applies. Thus, while the model deals well with the integrated effect of the distribution of the water vapor in the region up to ~10 km, it may not accurately model the *local* density of water vapor. This problem may be investigated by using Eq. (1) in the analysis of sky temperature measurements (Ref. 6).

IV. Summary and Conclusions

An exponential model of the water vapor pressure, $P_W(z) = P_{0W} \exp(-az - bz^2)$, has been shown to provide a good fit to radiosonde measurements of the wet-component tropospheric range error if a and b are functions of the surface temperature and pressure. The preliminary dependence of a and b on temperature and pressure has been deduced from 4 months of observations (Table 1 and Eq. 11). When the model of Table 1 is applied to the 4 months' data, the rms difference between the model and data is 1.4 cm. In the winter (December to April), when the wet component varies little, the monthly average should provide as good a fit to the data as the model.

References

1. Chao, C. C., 1972, "A New Method to Predict Zenith Range Correction From Surface Measurements," in *The Deep Space Network Progress Report*, Technical Report 32-1526, Vol. XIV, Jet Propulsion Laboratory, Apr. 15, 1973.
2. Winn, F. B., Montez, M., and Smock, G., *For MM71 Heliocentric Cruise: Tropospheric Refraction Models, Errors, Sensitivities as They Pertain to Radio Metric Doppler Fits*, TM 391-376, October 16, 1972 (JPL internal document).
3. Berman, A. L., "A New Tropospheric Range Refraction Model," in *The Deep Space Network*, Space Programs Summary 37-65, Vol. II, Nov. 30, 1970, p. 140.
4. Tverskoi, P. N., *Physics of the Atmosphere*, NASA Translation, U.S. Dept. of Commerce, Clearinghouse for Federal Scientific and Technical Information, Springfield, Va., 1962 (trans. 1965).
5. Thuleen, K. L., and Ondrasik, V. J., "The Repetition of Seasonal Variations in the Tropospheric Zenith Range Effect," in *The Deep Space Network Progress Report*, Technical Report 32-1526, Vol. VI, Jet Propulsion Laboratory, Dec. 15, 1971.
6. von Roos, O. H., *Preliminary Investigation of the Significance of Sky Temperature Measurements on the Determination of Water Vapor Properties in the Troposphere*, TM 391-418, March 2, 1973 (JPL internal document).

Table 1. Variation of model parameters *a* and *b* with surface temperature and pressure

Run	a, km^{-1}	b, km^{-2}	Effective scale height, km	Temperature range, °C	Pressure restrictions
XI	0.461	0.0768	2.61	0–13.0	–
IX	0.419	0.0658	2.85	13.1–18.5	–
VIII	0.329	0.0535	3.39	18.6–25.0	–
VIII	0.307	0.0502	3.54	25.0–30.0	$P_{0W} > 16.0 \times 10^2$ N/m^2
I	0.289	0.0480	3.71	25.1–32.4	$5.5 < P_{0W} \leq 16.0 \times 10^2$ N/m^2
VI	0.256	0.0461	3.96	32.5–35.0	$P_{0W} > 5.5 \times 10^2$ N/m^2
X	0.242	0.0404	4.21	35.1 up	$P_{0W} > 5.5 \times 10^2$ N/m^2
XII	0.200	0.0329	4.84	25.0 up	$P_{0W} \leq 5.5 \times 10^2$ N/m^2

Table 2. Summary of fit of model to radiosonde data

Data (1967)	Average ΔR_W, cm	Rms from average	Run	Bias[a], cm	Rms from model	Number of days	Temperature range, °C
April	3.55	0.76	IX	−0.30	0.92	20	1–20
			Combined	−0.22	0.72		
May	6.20	2.19	VIII	+0.41	1.91	27	12–32
			Combined	−0.06	1.32		
August	11.8	1.88	VI	+0.09	1.89	24	31–37
			Combined	−0.02	1.51		
September	10.8	3.60	I	+0.50	2.49	23	20–32
			Combined	+0.05	1.73		
All	–	–	Combined	−0.06	1.40	94	–
All, except April	–	–	Combined	−0.03	1.52	74	–

[a]Observed − computed.

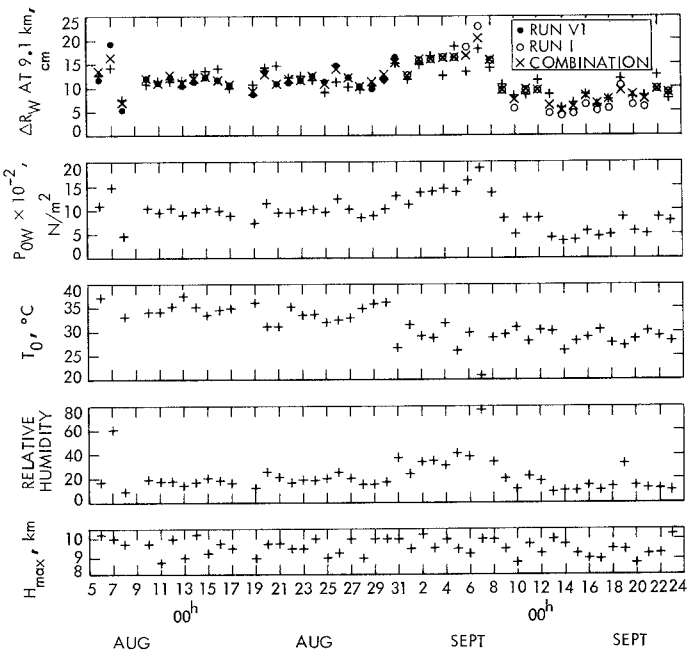

Fig. 1. Tropospheric data vs. date for August and September, 1967, Yucca Flats, Nevada; ΔR_W at 9.1 km, plotted with two models—best for each individual month and combination